Proceedings of the 1998 IEEE
International Conference on Robotics & Automation
Leuven, Belgium • May 1998

Motion/Force Decomposition of Redundant Manipulator and Its Application to Hybrid Impedance Control

Yonghwan Oh*, Wan Kyun Chung†, Youngil Youm‡ and Il Hong Suh§

Robotics Lab., School of Mech. Eng.,
Pohang University of Science & Technology(POSTECH)
Tel: +82-562-279-2844; Fax: +82-562-279-5899; e-mail:wkchung@postech.ac.kr/oyh@postech.ac.kr

Abstract

An approach to resolve the kinematic redundancy and to control the motion/force of redundant manipulators is presented. By defining a proper metric in joint space, minimal parameterization of motion and force controlled subspaces as well as the null motion component is realized. With this formulation, control of both motion/force and internal motion of redundant manipulator can be achieved via a new hybrid impedance control method with inertial decoupling of each space. Some numerical examples are given to demonstrate the performance of the proposed control method.

1 Introduction

The increasing demand for advanced manipulator applications has brought a numerous growth of interest in the development of different concepts and schemes for the control of compliant motion. Those can be classified into two approaches: the one is hybrid position/force control method and the other is the impedance control scheme. The advantages and limitations on these schemes are well described in [4, 9]. Among the many control algorithms, hybrid impedance control method has been reported as an unified approach to compliant control[1, 5]. Recently, the extensions of such approach to redundant manipulators were proposed in the literatures[6, 8]. These compliant motion tasks can be performed more smoothly if we use redundant degrees of freedom like human arm and fingers. In joint space, there is no distinction of the dynamics between redundant and non-redundant manipulators. However, if the manipulator motion is defined by the task of its end-effector and when we express the dynamics in task space, the dynamics of remaining degrees of freedom does not appear in this formulation[3]. Thus, in order to take a full advantage of the redundancy, dealing with the hidden internal dynamics is essential for achieving higher performance of both position and compliant motions because the hidden dynamics affects the task space motions of redundant manipulators.

The motivation of this paper is to provide a method to express the behavior of redundant manipulators with task and null space dynamics with decoupled manner using appropriate decomposition method.

2 Kinestatic Modeling and Task Space Decomposition

Kinematic redundancy in manipulator gives rise to two aspects of problem[3]: One is the motion redundancy and the other is the force redundancy. It should be noted here that in order to achieve better performance of redundant manipulators, it is necessary to express the motion of manipulator including null space dynamics[6, 7]. Moreover, it would be better if we have separate control on both task and null space motions, independently.

2.1 Kinestatic Modeling and Minimal Null Space Parameterization

Consider an n-DOF serial manipulator operating in an m-dimensional Cartesian coordinates. Its kinematics is expressed by the following three equations

$$\mathbf{x} = \mathbf{k}(\mathbf{q}) \tag{1a}$$

$$\dot{\mathbf{x}} = \mathbf{J}(\mathbf{q})\dot{\mathbf{q}}, \quad \mathbf{J}(\mathbf{q}) = \frac{\partial \mathbf{k}(\mathbf{q})}{\partial \mathbf{q}^T} \tag{1b}$$

$$\ddot{\mathbf{x}} = \mathbf{J}(\mathbf{q})\ddot{\mathbf{q}} + \mathbf{h}(\mathbf{q}, \dot{\mathbf{q}}), \quad \mathbf{h}(\mathbf{q}, \dot{\mathbf{q}}) \triangleq \dot{\mathbf{J}}(\mathbf{q}, \dot{\mathbf{q}})\dot{\mathbf{q}}, \tag{1c}$$

where $\mathbf{k}(\cdot) : \Re^n \rightarrow \Re^m$ is the forward kinematics; $\dot{\mathbf{q}} \in \mathcal{Q} \subset \Re^n$ is the generalized joint velocity; $\dot{\mathbf{x}} \in \mathcal{X} \subset \Re^m$

* Ph.D student, POSTECH
† Associate Professor, POSTECH
‡ Professor, POSTECH
§ Professor, Hanyang Univ.

is the Cartesian end-effector velocity; $\mathbf{J} \in \Re^{m \times n}$ denotes the manipulator Jacobian matrix and $r = n - m(n > m)$ is called the degree-of-redundancy.

Usually kinematic problem of redundant manipulator is to find the solution of Eq. (1b). When the manipulator has both prismatic and revolute joints, the frequently used Moore-Penrose inverse of $\mathbf{J}$ lacks the physical meaning and it is not invariant with change of measure units to describe the structure [2, 3, 4].

In this case, it is more reasonable to define the norm of $\dot{\mathbf{q}}$ with a metric $\mathbf{W}$

$$\|\dot{\mathbf{q}}\|_W^2 = \dot{\mathbf{q}}^T \mathbf{W} \dot{\mathbf{q}}. \tag{2}$$

Then the minimum norm solution of Eq. (1b) is obtained by

$$\dot{\mathbf{q}} = \mathbf{J}_W^+ \dot{\mathbf{x}}, \quad \mathbf{J}_W^+ \triangleq \mathbf{W}^{-1}\mathbf{J}^T \left(\mathbf{J}\mathbf{W}^{-1}\mathbf{J}^T\right)^{-1} \tag{3}$$

where $\mathbf{J}_W^+$ denotes the weighted pseudo-inverse. From this, we can naturally induce a Cartesian space metric $\mathbf{M}$ using Eq. (2) as follows

$$\dot{\mathbf{q}}^T \mathbf{W} \dot{\mathbf{q}} = \dot{\mathbf{x}}^T \mathbf{J}_W^{+T} \mathbf{W} \mathbf{J}_W^+ \dot{\mathbf{x}} = \dot{\mathbf{x}}^T \mathbf{M} \dot{\mathbf{x}} \tag{4}$$

where $\mathbf{M} \triangleq (\mathbf{J}\mathbf{W}^{-1}\mathbf{J}^T)^{-1}$. Since Eq. (3) shows the minimum norm solution only, it is not a full parameterization of the joint motion. Thus the full decomposition of $\dot{\mathbf{q}}$ can be given by:

$$\dot{\mathbf{q}} = \dot{\mathbf{q}}_p + \dot{\mathbf{q}}_h = \mathbf{J}_W^+ \dot{\mathbf{x}} + \left(\mathbf{I}_n - \mathbf{J}_W^+ \mathbf{J}\right) \boldsymbol{\xi}, \tag{5}$$

where $\dot{\mathbf{q}}_h = \left(\mathbf{I}_n - \mathbf{J}_W^+ \mathbf{J}\right) \boldsymbol{\xi} \in \mathcal{N}(\mathbf{J})$ denotes the homogeneous solution of Eq. (1b) which represents the internal or null space motion and $\boldsymbol{\xi} \in \Re^n$ is an arbitrary vector. However, the above matrix $\left(\mathbf{I}_n - \mathbf{J}_W^+ \mathbf{J}\right)$ does not behave as a projection matrix because it does not have symmetric and idempotent properties. $\dot{\mathbf{q}}_p$ and $\dot{\mathbf{q}}_h$ do not satisfy the orthogonal condition but weighted orthogonal property.

With an arbitrary choice of $\boldsymbol{\xi}$, the homogeneous solution can be written as[7]

$$\dot{\mathbf{q}}_h = \left(\mathbf{I}_n - \mathbf{J}_W^+ \mathbf{J}\right) \boldsymbol{\xi} = \mathbf{V}(\mathbf{q}) \dot{\mathbf{x}}_N, \tag{6}$$

where $\mathbf{V} \in \Re^{n \times r}$ is a set of linearly independent vectors which spans the null space of $\mathbf{J}$ and $\dot{\mathbf{x}}_N \in \mathcal{X}_N$ denotes r-dimensional minimal parameters of $\mathcal{N}(\mathbf{J})$. Using Eqs. (5) and (6), we obtain $\dot{\mathbf{x}}_N$:

$$\dot{\mathbf{x}}_N = \left(\mathbf{V}^T \mathbf{W} \mathbf{V}\right)^{-1} \mathbf{V}^T \mathbf{W} \dot{\mathbf{q}} \triangleq \mathbf{J}_N(\mathbf{q}) \dot{\mathbf{q}}. \tag{7}$$

Similar to the decomposition of joint velocities $\dot{\mathbf{q}}$, the joint torque vector can be characterized as follows:

$$\boldsymbol{\tau} = \boldsymbol{\tau}_p + \boldsymbol{\tau}_h = \mathbf{J}^T \mathbf{f}_c + \left(\mathbf{I}_n - \mathbf{J}^T \mathbf{J}_W^{+T}\right) \boldsymbol{\gamma}_n, \tag{8}$$

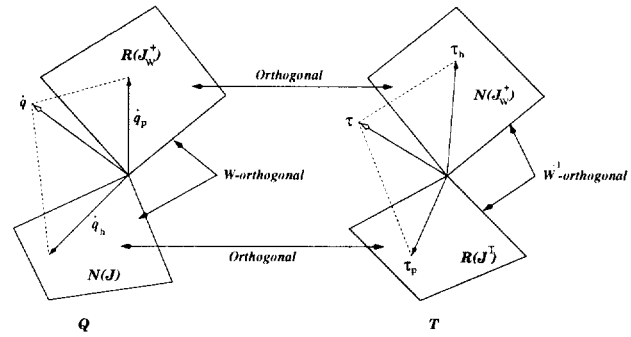

Fig. 1: Weighted joint space decomposition

where $\mathbf{f}_c \in \Re^m$ denotes the command force vector in Cartesian coordinates and $\boldsymbol{\gamma}_n \in \Re^n$ is an arbitrary vector. Similar to $\dot{\mathbf{q}}_h$, $\boldsymbol{\tau}_h$ is the homogeneous torques which does not contribute to the end-effector motion.

Clearly, $\boldsymbol{\tau}_p$ and $\boldsymbol{\tau}_h$ are not orthogonal but weighted orthogonal, and weighting matrix is $\mathbf{W}^{-1}$ to satisfy the consistency. From the duality of Eq. (7), we rewrite $\boldsymbol{\tau}_h$ as follows:

$$\boldsymbol{\tau}_h = \left(\mathbf{I}_n - \mathbf{J}^T \mathbf{J}_W^{+T}\right) \boldsymbol{\gamma}_n = \mathbf{J}_N^T \mathbf{f}_N, \tag{9}$$

where $\mathbf{f}_N \in \Re^r$ denotes the null space force which gives rise to the null motion $\dot{\mathbf{x}}_N$. Fig. 1 shows the above decomposition of joint space based on the above analysis. This is very similar to the twist-wrench kinestatic filter and each reciprocal product is always zero[4].

2.2 Task Space Decomposition

Usually, many tasks to be performed by manipulator require the geometrical information of the environment in task space and the description of dynamics in that space is helpful in designing the control method. For instance, the manipulator can be commanded to exert desired force to some directions of the constraint surface while moving to other directions. By defining a task frame at the end-effector, description of such task can be simplified and the task frame should be identified according to the given task[5, 6].

For compliant motion control problem, typical tasks can be divided by two classes: The first one is the non-tracking task frame, *i.e.*, the task frame directions remain fixed to either the manipulated object-such as in peg-in-hole case or the environment. The second one is the tracking task frame, *i.e.*, the task frame's update is directly derived from the constraint model or sensor measurements.

In either cases, the following non-holonomic constraint form can be considered

$$\dot{\mathbf{r}}_F = \mathbf{E}_F(\mathbf{x}) \dot{\mathbf{x}}, \quad \mathbf{E}_F \in \Re^{k \times m} \tag{10}$$

and assume that $\mathbf{E}_F$ is a full row rank matrix. In most results of hybrid control, the assumption that the manipulator in contact can be represented by a mechanical system model subjected to the ideal constraints was explicitly or implicitly used[4, 6, 9]. If we consider such ideal constraints, then $\mathbf{r}_F = \dot{\mathbf{r}}_F = \mathbf{0}$. However, due to the local deformation occurred at the contact point, velocity of the end-effector pointing into the constraint surface is nonzero. $\dot{\mathbf{r}}_F$ in Eq. (10) can be used for such situation.

If Eq. (10) is a Jacobian matrix of the holonomic constraint, *i.e.*, $\mathbf{E}_F\dot{\mathbf{x}}$ is integrable, then we obtain

$$\mathbf{r}_F = \boldsymbol{\phi}(\mathbf{x}), \quad \boldsymbol{\phi}(\mathbf{x}) \in \Re^k$$

where $k \leq m$ and in this case, $\mathbf{E}_F$ is given by

$$\mathbf{E}_F(\mathbf{x}) = \frac{\partial \boldsymbol{\phi}(\mathbf{x})}{\partial \mathbf{x}^T}. \tag{11}$$

Typical example of the above equation is the contour following problem. In Eq. (10), each row of $\mathbf{E}_F$ is neither orthogonal nor normalized. Note that the conventional hybrid control schemes[4] can not be applied to the case in which the orthogonal task frame is not defined.

From Eq (10), we know that

$$\dot{\mathbf{x}} = \left(\mathbf{I}_m - \mathbf{E}_{FM}^{+}\mathbf{E}_F\right)\dot{\mathbf{x}} + \mathbf{E}_{FM}^{+}\dot{\mathbf{r}}_F, \tag{12}$$

where $\mathbf{E}_{FM}^{+}$ is the weighted generalized inverse of $\mathbf{E}_F$:

$$\mathbf{E}_{FM}^{+} = \mathbf{M}^{-1}\mathbf{E}_F^T\left(\mathbf{E}_F\mathbf{M}^{-1}\mathbf{E}_F^T\right)^{-1}$$

and $\mathbf{M}$ denotes the Cartesian space metric which is induced from the joint space metric as mentioned before.

Similar to the joint space decomposition in the previous section, let us define a set of null space basis of $\mathbf{E}_F$ as $\mathbf{N}$, *i.e.*, $\mathbf{E}_F\mathbf{N} = \mathbf{0}$, then the Cartesian motion system of Eq. (12) has the following form:

$$\dot{\mathbf{x}} = \mathbf{N}\dot{\mathbf{r}}_P + \mathbf{E}_{FM}^{+}\dot{\mathbf{r}}_F, \tag{13}$$

where $\dot{\mathbf{r}}_P \in \Re^{m-k}$ is the minimal parameter of $\mathcal{N}(\mathbf{E}_F)$. Since $\mathbf{N}$ has the full-column rank, we get $\dot{\mathbf{r}}_P$ as follows using the Cartesian metric $\mathbf{M}$:

$$\dot{\mathbf{r}}_P = \left(\mathbf{N}^T\mathbf{M}\mathbf{N}\right)^{-1}\mathbf{N}^T\mathbf{M}\dot{\mathbf{x}} \triangleq \mathbf{E}_P(\mathbf{q})\dot{\mathbf{x}}. \tag{14}$$

Augmenting Eqs. (10) and (14), we get

$$\dot{\mathbf{r}} = \begin{Bmatrix} \dot{\mathbf{r}}_P \\ \dot{\mathbf{r}}_F \end{Bmatrix} = \begin{bmatrix} \mathbf{E}_P \\ \mathbf{E}_F \end{bmatrix}\dot{\mathbf{x}} = \mathbf{R}(\mathbf{x})\dot{\mathbf{x}}, \tag{15}$$

where $\mathbf{R} \in \Re^{m\times m}$ denotes the transformation matrix from the Cartesian coordinates to the task space coordinates.

From the duality of Eq. (10), we get the Cartesian force system of the form:

$$\mathbf{f} = \mathbf{E}_P^T\boldsymbol{\lambda}_P + \mathbf{E}_F^T\boldsymbol{\lambda}_F = \mathbf{R}^T(\mathbf{x})\boldsymbol{\lambda}. \tag{16}$$

In the above equation, $\mathbf{E}_F^T$ constitutes a basis of the active force controlled subspace and $\boldsymbol{\lambda}_F \in \Re^k$ denotes the parameter vector in that space. Each parameter $\boldsymbol{\lambda}_P$ and $\boldsymbol{\lambda}_F$ can be found by

$$\begin{aligned} \boldsymbol{\lambda}_P &= \mathbf{N}^T\mathbf{f} \\ \boldsymbol{\lambda}_F &= \mathbf{E}_{FM}^{+T}\mathbf{f}. \end{aligned} \tag{17}$$

When the frictionless contact is considered, $\boldsymbol{\lambda}_P = \mathbf{0}$.

3 A New Extended Task Space Formulation

When the manipulator contacts with the environment, its equations of motion in joint space can be given by

$$\boldsymbol{\tau} = \mathbf{H}(\mathbf{q})\ddot{\mathbf{q}} + \mathbf{C}(\mathbf{q},\dot{\mathbf{q}})\dot{\mathbf{q}} + \mathbf{g}(\mathbf{q}) + \mathbf{J}^T(\mathbf{q})\mathbf{f}, \tag{18}$$

where $\mathbf{H}(\mathbf{q}) \in \Re^{n\times n}$ is the symmetric and positive definite joint inertia matrix; $\mathbf{C}(\mathbf{q},\dot{\mathbf{q}})\dot{\mathbf{q}} \in \Re^n$ involves Coriolis and centrifugal terms; $\mathbf{g}(\mathbf{q}) \in \Re^n$ denotes gravity force; $\boldsymbol{\tau} \in \Re^n$ is the generalized joint torque vector; $\mathbf{f} \in \Re^m$ is the contact force exerted by the end-effector on the environment in Cartesian coordinates.

3.1 Extended Task Space Formulation

Now, we want to describe the dynamics of redundant manipulator in task space. Normally dynamic description of the redundant manipulator in task space[3] has a drawback in the sense of missing of the hidden internal motion dynamics, because the null motion does not affect the motion of end-effector in velocity level. However, through the strong dynamic coupling between them, those affect each other in acceleration level. This is the reason why we need to express the null space dynamics explicitly[7]. This will be possible using the following minimal parameterization of null space motion.

Hereafter, we assume the kinetic energy metric[2, 7], *i.e.*, $\mathbf{W} = \mathbf{H}(\mathbf{q})$. Let us define the extended task space variables as follows:

$$\dot{\mathbf{x}}_E = \left(\dot{\mathbf{r}}_P^T \;\; \dot{\mathbf{r}}_F^T \;\; \dot{\mathbf{x}}_N^T\right)^T. \tag{19}$$

Then, we obtain the following relations:

$$\begin{aligned} \dot{\mathbf{x}}_E &= \mathbf{J}_E\dot{\mathbf{q}} \\ \ddot{\mathbf{x}}_E &= \mathbf{J}_E\ddot{\mathbf{q}} + \mathbf{h}_E(\mathbf{q},\dot{\mathbf{q}}), \end{aligned} \tag{20}$$

where

$$\mathbf{J}_E(\mathbf{q}) = \begin{bmatrix} \mathbf{J}_P(\mathbf{q}) \\ \mathbf{J}_F(\mathbf{q}) \\ \mathbf{J}_N(\mathbf{q}) \end{bmatrix} = \begin{bmatrix} \mathbf{E}_P\mathbf{J} \\ \mathbf{E}_F\mathbf{J} \\ \mathbf{J}_N \end{bmatrix} \text{ and}$$
$$\mathbf{h}_E(\mathbf{q},\dot{\mathbf{q}}) = \begin{pmatrix} \mathbf{h}_P(\mathbf{q},\dot{\mathbf{q}}) \\ \mathbf{h}_F(\mathbf{q},\dot{\mathbf{q}}) \\ \mathbf{h}_N(\mathbf{q},\dot{\mathbf{q}}) \end{pmatrix} = \begin{pmatrix} \dot{\mathbf{J}}_P\dot{\mathbf{q}} \\ \dot{\mathbf{J}}_F\dot{\mathbf{q}} \\ \dot{\mathbf{J}}_N\dot{\mathbf{q}} \end{pmatrix}. \quad (21)$$

In Eq. (20), $\mathbf{J}_E$ is an extended Jacobian matrix and its inverse is given by

$$\mathbf{J}_E^{-1} = \begin{bmatrix} \mathbf{J}_H^+\mathbf{N} & \mathbf{J}_{FH}^+ & \mathbf{V} \end{bmatrix}. \quad (22)$$

From the principle of virtual work, we know that

$$\boldsymbol{\tau} = \mathbf{J}_E^T(\mathbf{q})\boldsymbol{\lambda}_{Ec}, \quad (23)$$

where

$$\boldsymbol{\lambda}_{Ec} = \begin{pmatrix} \boldsymbol{\lambda}_{Pc}^T & \boldsymbol{\lambda}_{Fc}^T & \mathbf{f}_N^T \end{pmatrix}^T \text{ and } \boldsymbol{\lambda}_E = \begin{pmatrix} \boldsymbol{\lambda}_P^T & \boldsymbol{\lambda}_F^T & \mathbf{0} \end{pmatrix}.$$

Using the above equations, we can obtain the dynamic equations of motion in extended task space as follows:

$$\boldsymbol{\lambda}_{Ec} = \boldsymbol{\Lambda}_{ET}\ddot{\mathbf{x}}_E + \boldsymbol{\Gamma}_{ET}(\mathbf{q},\dot{\mathbf{q}})\dot{\mathbf{x}}_E + \boldsymbol{\eta}_{ET} + \boldsymbol{\lambda}_E. \quad (24)$$

In this equation,

$$\boldsymbol{\Lambda}_{ET}(\mathbf{q}) = \begin{bmatrix} \boldsymbol{\Lambda}_P(\mathbf{q}) & \mathbf{0} & \mathbf{0} \\ \mathbf{0} & \boldsymbol{\Lambda}_F(\mathbf{q}) & \mathbf{0} \\ \mathbf{0} & \mathbf{0} & \boldsymbol{\Lambda}_N(\mathbf{q}) \end{bmatrix}$$
$$\boldsymbol{\Gamma}_{ET}(\mathbf{q},\dot{\mathbf{q}}) = \mathbf{J}_E^{-T}\left\{\mathbf{C}(\mathbf{q},\dot{\mathbf{q}}) - \mathbf{H}(\mathbf{q})\mathbf{J}_E^{-1}\dot{\mathbf{J}}_E\right\}\mathbf{J}_E^{-1}$$
$$\boldsymbol{\eta}_{ET}(\mathbf{q}) = \mathbf{J}_E^{-T}\mathbf{g}(\mathbf{q}),$$

where $\boldsymbol{\Lambda}_P(\mathbf{q}) \triangleq \mathbf{N}^T\boldsymbol{\Lambda}\mathbf{N}$, $\boldsymbol{\Lambda}_F(\mathbf{q}) \triangleq (\mathbf{J}_F\mathbf{H}^{-1}\mathbf{J}_F^T)^{-1}$ and $\boldsymbol{\Lambda}_N(\mathbf{q}) = \mathbf{V}^T\mathbf{H}\mathbf{V}$[7]. Because of the weighting matrix $\mathbf{W} = \mathbf{H}(\mathbf{q})$, there is no coupling effect between the null space and task space in inertia term[7].

Usually, there has been no separate control on null dynamics which is coupled with that of task space motion, the fail of control on null space generally degrades the performance of task space motion. This neat decoupled dynamic property will be used in designing the extended hybrid impedance control scheme in the next section.

4 Extended Hybrid Impedance Controller

Hybrid impedance control method combines hybrid position/force control and impedance control into one scheme[1, 5, 6]. Fig. 2 shows the fundamental idea of the control scheme. As denoted in the figure, the main objective of the hybrid impedance control method is to make the behavior of the manipulator like mass-spring-damper system for impedance controlled direction and mass-damper system for force controlled direction.

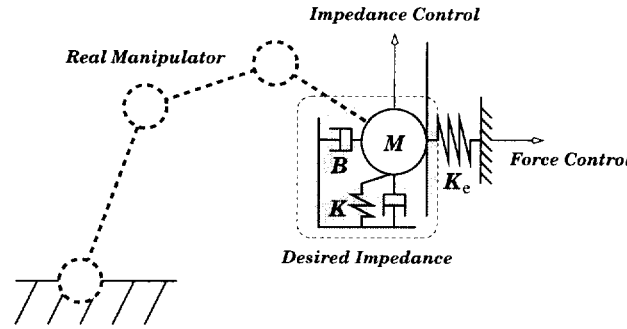

Fig. 2: Fundamental idea of hybrid impedance control

4.1 Inertially Decoupled Extended Hybrid Impedance Control Method

The target impedance relations of each space can be given by

$$\begin{aligned} \mathbf{M}_{Pd}\ddot{\mathbf{e}}_P + \mathbf{B}_{Pd}\dot{\mathbf{e}}_P + \mathbf{K}_{Pd}\mathbf{e}_P &= \mathbf{0} \\ \mathbf{M}_{Fd}\ddot{\mathbf{r}}_F + \mathbf{B}_{Fd}\dot{\mathbf{r}}_P &= \alpha_F\mathbf{e}_F \\ \mathbf{M}_{Nd}\ddot{\mathbf{e}}_N + \mathbf{B}_{Nd}\dot{\mathbf{e}}_N &= \mathbf{0}. \end{aligned} \quad (25)$$

In the above, $\mathbf{M}_{(\cdot)}$, $\mathbf{B}_{(\cdot)}$ and $\mathbf{K}_{Pd}$ denote the desired impedance parameters in each space, $\mathbf{e}_P = \mathbf{r}_{Pd} - \mathbf{r}_P$; $\mathbf{e}_F = \boldsymbol{\lambda}_{Fd} - \boldsymbol{\lambda}_F$; $\dot{\mathbf{e}}_N = \dot{\mathbf{x}}_{Nd} - \dot{\mathbf{x}}_N$ and $\alpha_F > 0$. Then based on the proposed formulation, we obtain the following controller for motion/force of the end-effector as well as null motion of the redundant manipulator:

$$\boldsymbol{\tau} = \boldsymbol{\tau}_P + \boldsymbol{\tau}_F + \boldsymbol{\tau}_N + \mathbf{C}(\mathbf{q},\dot{\mathbf{q}})\dot{\mathbf{q}} + \mathbf{g}(\mathbf{q}) + \mathbf{J}^T\mathbf{f}, \quad (26)$$

where $\boldsymbol{\tau}_P$, $\boldsymbol{\tau}_F$ denote the command torques for motion and force controlled subspaces and $\boldsymbol{\tau}_N$ is the null space command torques. Those have the following form:

$$\begin{aligned} \boldsymbol{\tau}_P &= \mathbf{J}^T\boldsymbol{\Lambda}\mathbf{N}\left\{\ddot{\mathbf{r}}_{Pd} + \mathbf{M}_{Pd}^{-1}(\mathbf{B}_{Pd}\dot{\mathbf{e}}_P + \mathbf{K}_{Pd}\mathbf{e}_P) - \mathbf{h}_P\right\} \\ \boldsymbol{\tau}_F &= \mathbf{J}_F^T\boldsymbol{\Lambda}_F\left\{\mathbf{M}_{Fd}^{-1}(\alpha_F\mathbf{e}_F - \mathbf{B}_{Fd}\dot{\mathbf{r}}_F) - \mathbf{h}_F\right\} \\ \boldsymbol{\tau}_N &= \mathbf{H}\mathbf{V}\left\{\ddot{\mathbf{x}}_{Nd} + \mathbf{M}_{Nd}^{-1}\mathbf{B}_{Nd}\dot{\mathbf{e}}_N - \mathbf{h}_N\right\}. \end{aligned}$$

Proposition 1. *Applying Eq. (26) to Eq. (24), we obtain the desired impedance relation given by Eq. (25). Moreover, we get* $\mathbf{e}_P \to \mathbf{0}$, $\dot{\mathbf{e}}_N \to \mathbf{0}$ *and* $\mathbf{e}_F \to \mathbf{0}$.

PROOF. Since the closed loop systems of motion controlled subspace and null space given in Eq.(25) satisfy the desired objectives directly, only the stability of force controlled subspace is considered. Let's take a set of state of the form:

$$\mathbf{z}_1 = \mathbf{r}_F - \mathbf{r}_{Fd}, \;\; \mathbf{z}_2 = \dot{\mathbf{r}}_F \tag{27}$$

and consider a Lyapunov function candidate of the form:

$$V(\mathbf{z}_1, \mathbf{z}_2) = \frac{1}{2}\mathbf{z}_2^T \mathbf{M}_{Fd}\mathbf{z}_2 + \alpha_F \sum_{i=1}^{k} \Psi_i(\mathbf{z}_1) \tag{28}$$

where Ψ_i is given by

$$\Psi_i(\mathbf{z}_1) = \int^{z_{1,i}} [\lambda_{F,i}(r_{Fd,i} + \zeta) - \lambda_{Fd,i}]\, d\zeta.$$

Then time derivatives of the above equation is

$$\dot{V} = -\mathbf{z}_2^T \mathbf{B}_{Fd}\mathbf{z}_2 \leq 0. \tag{29}$$

$\mathbf{z}_2 = \mathbf{0}$ implies $\dot{\mathbf{z}}_2 = \mathbf{0}$. Then from Eq. (25), we know that $\mathbf{e}_F = \mathbf{0}$ and it implies $\mathbf{z}_1 = \mathbf{r}_F - \mathbf{r}_{Fd} = \mathbf{0}$. Therefore, we can achieve that $\boldsymbol{\lambda}_F \to \boldsymbol{\lambda}_{Fd}$ as $t \to \infty$. □

5 Simulation

In this section, we show the performance of the proposed controller by computer simulations. A three-link planar redundant manipulator is considered in the simulation study. For simplicity, the joint friction torques are neglected. For all simulations, the sampling frequency is assumed as 500Hz.

Since the degrees of redundancy is one in this case, the null space motion can be characterized by a scalar quantity. To achieve secondary task, we use the manipulability as a performance index $m(\mathbf{q})$ with scaling. The desired null motion $\dot{\mathbf{x}}_{Nd}$ is given by the gradient projection method[7] of the form:

$$\dot{\mathbf{x}}_{Nd} = \kappa \boldsymbol{\Lambda}_N^{-1} \mathbf{V}^T \nabla m(\mathbf{q}), \tag{30}$$

where κ denotes the rate of convergent factor. In this paper, we use $\kappa = 1$ and $B_N = 0.03$. We choose $\mathbf{M}_{Fd} = \boldsymbol{\Lambda}_F(\mathbf{q})$, $\mathbf{M}_{Pd} = \boldsymbol{\Lambda}_P(\mathbf{q})$ and $\mathbf{M}_{Nd} = \boldsymbol{\Lambda}_N(\mathbf{q})$[7]. The other terms are $\alpha_F = 0.8$, $B_{Pd} = 60$ and $B_{Fd} = 100$.

5.1 Compliant Motion Control

The primary task is to follow the desired end-effector trajectory which is a line segment from (0.2, 0)m to (0.6, 0)m in Cartesian space while exerting a desired contact force $\lambda_{Fd} = 20$ to the environment. The manipulator

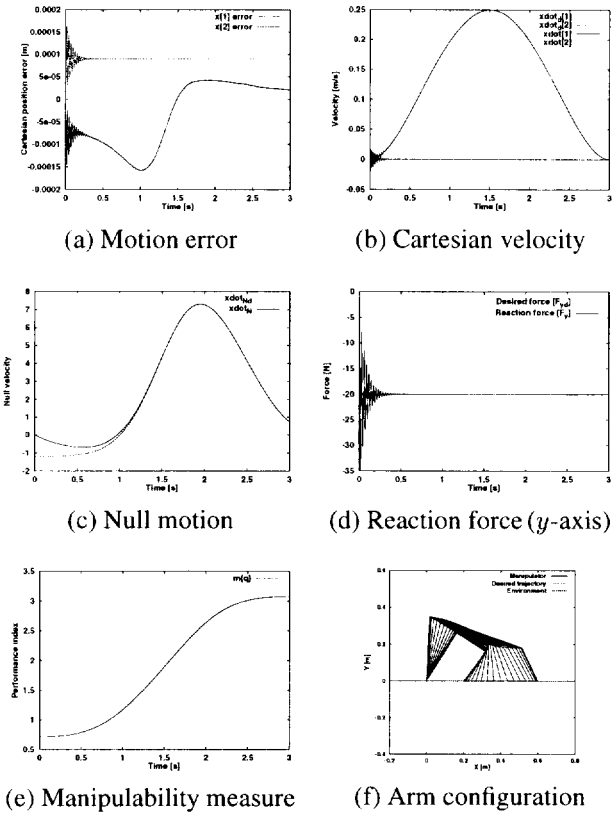

(a) Motion error (b) Cartesian velocity

(c) Null motion (d) Reaction force (y-axis)

(e) Manipulability measure (f) Arm configuration

Fig. 3: Compliant motion control performance

is assumed to be in contact with the environment at initial time with small pre-load force and a holonomic constraint form of environment is considered as follows:

$$y = 0. \tag{31}$$

We consider a spring like contact force model, *i.e.*, $\lambda_F = K_e \delta r_F$ and K_e is give by 200,000N/m. The total time of execution is given by 3s. Fig. 3 shows the simulation result of the proposed control method. As shown in Figs. 3(a) and (b), the manipulator tracks the desired Cartesian motion to the unconstrained direction. Whereas the null motion tracking performance and the force control performance is also good as illustrated in Figs. 3(c) and (d). As shown in Fig. 3(d), it shows very oscillatory performance at initial time. The reason is that within the proposed formulation, the manipulator behaves like a mass-damper system model. Since we assumed spring like contact force model with high stiffness, the total system shows the under-damped mass-spring-damper system behavior. Fig. (e) shows the change of the manipulability measure and Fig. (f) is some snapshots of the manipulator during the task execution.

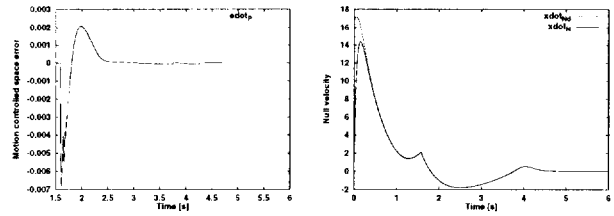

(a) $\dot{\mathbf{e}}_P$ (b) Null motion

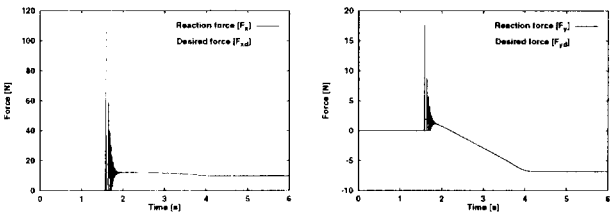

(c) x-axis force (d) y-axis force

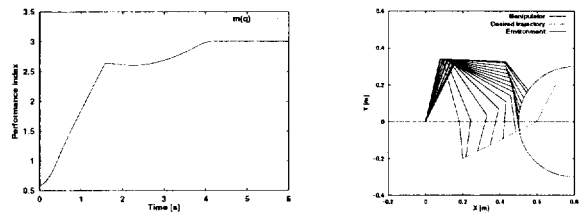

(e) Manipulability measure (f) Arm configuration

Fig. 4: Contact transition control performance

5.2 Contact Motion Control

In this section, we investigate the performance of the proposed extended hybrid impedance controller for a general class of task execution, *i.e.,* free, contact and compliant motion. The desired trajectory is given by two straight line segments in the Cartesian space with fifth order polynomial of time. A circular environment of which center is (0.8, 0) with radius of 0.3m is considered. When the contact force is nonzero, the control mode switching occurred and the normal contact force λ_{Fd} is given by 20. Note that $\|\lambda_{Fd}\|_{\Lambda_F^{-1}} = \|\mathbf{f}_d\|_{\Lambda^{-1}}$. An arbitrary initial configuration is chosen and the total execution time is given by 5s. Fig. 4 shows the simulation results. As observed in Figs. 4(a)-(d), the manipulator shows good position tracking performance and makes stable contact with the environment after initial transient period. Moreover, it shows good force tracking performance after contact. Notice that the null-motion is not seriously affected by the impact situation as shown in Fig. 4(b). This can not be obtained in conventional extended task space methods because of the inertial coupling. Since initial configuration of the manipulator is not an optimal, there exists non-zero initial null motion velocity. Figs. 4(e) and (f) show the performance index and manipulator configuration during the task execution, respectively.

6 Conclusion

In this paper, we addressed the decomposition of the redundant manipulators for controlling motion/force of the end-effector as well as the internal motion. From the weighted decomposition of the joint space, we derived the full space decomposition of redundant manipulators. The proposed extended task space formulation enable us to design the control methods of each space independently. Embedding the hybrid impedance control approach to the proposed formulation, we obtained the inertially decoupled extended hybrid impedance control law (ExHIC) and its stability proof was shown. Those analyses were verified through the numerical simulations for stiff environment with a planar redundant manipulator.

REFERENCES

[1] R. J. Anderson and M. W. Spong, "Hybrid Impedance Control of Robotic Manipulators," *IEEE J. of Robotics and Automation*, vol. 4, No. 5, pp. 549–556, Oct., 1988

[2] K. L. Doty, C. Melchiorri and C. Bonivento, "A Theory of Generalized Inverse Applied to Robotics," *Int. J. of Robotics Research*, vol. 12, No. 1, pp. 1–19, Feb., 1993

[3] O. Khatib, "Motion/Force Redundancy of Manipulators," *JAPAN–USA. Symp. on Flexible Automation*, pp. 337–342, 1990

[4] H. Lipkin and J. Duffy, "Hybrid Twist and Wrench Control for a Robotic Manipulators," *Trans. of the ASME J. of Mechanisms, Transmission, and Automation in Design*, vol. 110, pp. 138–144, Jun., 1988

[5] G. J. Liu and A. A. Goldenberg, "Robust Hybrid Impedance Control of Robot Manipulators," *Proc. of IEEE Int. Conf. on Robotics and Automation*, pp. 287–292, 1991

[6] Y. Oh, W. K. Chung and Y. Youm, "General Task Execution of Redundant Manipulators with Explicit Null-Motion Control," *Proc. of IEEE Int. Conf. on Industrial Electronics*, pp. 1902–1908, 1996

[7] Y. Oh, W. K. Chung and Y. Youm, "Extended Impedance Control of Redundant Manipulators Using Joint Space Decomposition," *Proc. of IEEE Int. Conf. on Robotics and Automation*, pp. 1080–1087, 1997

[8] Z. X. Peng and N. Adachi, "Compliant Motion Control of Kinematically Redundant Manipulators," *IEEE Trans. on Robotics and Automation*, vol. 9, No. 6, pp. 831–837, Dec., 1993

[9] M. Vukobratović and R. Stojić, "Historical Perspective of Hybrid Control in Robotics: Beginning, Evolution, Criticism and Trends," *J. of Mech. Mach. Theory*, vol. 30, No. 4, pp. 519–532, 1995